Electrochemistry in Room-Temperature Ionic Liquids: Potential Windows at Mercury Electrodes

Emma I. Rogers,[†] Biljana Šljukić,[‡] Christopher Hardacre,[§] and Richard G. Compton*,[†]

Department of Chemistry, Physical and Theoretical Chemistry Laboratory, Oxford University, South Parks Road, Oxford OX1 3QZ, United Kingdom, Faculty of Physical Chemistry, University of Belgrade, Studentski trg 12, 11000 Belgrade, Serbia, and School of Chemistry and Chemical Engineering/QUILL, Queen's University Belfast, Belfast, Northern Ireland BT9 5AG, United Kingdom

The cathodic and anodic potential limits of eleven different ionic liquids were determined at a mercury hemisphere electrode. Ionic liquids containing the phosphonium cation (tri(*n*-hexyl)tetradecylphosphonium, $[P_{14,6,6,6}]^+$) give the largest potential window, especially when coupled to a trifluorotris(pentafluoroethyl)-phosphate, $[FAP]^-$, or bis(trifluoromethanesulfonyl)imide, $[NTf_2]^-$, anion.

1. Introduction

Room-temperature ionic liquids (RTILs) are composed entirely of ions, usually a bulky organic cation and an organic/inorganic anion, and they exist in the liquid state at or around 298 K. The abundance of charge-carrying ions allows for their use as solvents without the need for supporting electrolyte, and the chemical robustness of the ions lead to high thermal and chemical stability and large electrochemical potential windows (ca. (4.5 to 6.0) V). ILs are more environmentally friendly than volatile organic solvents because of their near-zero volatility, suggesting that they are an attractive substitute for conventional solvents for use in electrochemistry.[1−4]

The combination of different cations and anions has been shown to influence the properties exhibited by these liquids, including viscosity, density, conductivity, melting and decomposition temperatures, and hydrophobicity/hydrophilicity,[1−4] and this has recently been reviewed by O'Mahony et al.[5] In addition to the aforementioned properties, it has been reported that the reduction and oxidation of the cationic and anionic components, respectively, determine the cathodic and anodic limits observed,[6−8] thus establishing a range within which RTILs can be used in electrochemical applications.

The electrochemical potential window of ionic liquids has been studied[6] on a platinum electrode, and a general trend was observed for the magnitude of the potential window following the RTIL sequence $[P_{14,6,6,6}][FAP] > [N_{6,2,2,2}][NTf_2] > [C_6mim][FAP] > [C_2mim][NTf_2]$ (where $[P_{14,6,6,6}]^+$ = tri(*n*-hexyl)tetradecylphosphonium, $[N_{6,2,2,2}]^+$ = *n*-hexyltriethylammonium, $[C_6mim]^+$ = 1-hexyl-3-methylimidazolium, $[C_2mim]^+$ = 1-ethyl-3-methylimidazolium, $[FAP]^-$ = trifluorotris-(pentafluoroethyl)phosphate and $[NTf_2]^-$ = bis(trifluoromethanesulfonyl)imide), suggesting that the size of the potential window is affected not only by the identity of the cations and anions but also by the particular combinations of the ionic substituents.

It has been shown that the electrochemical potential window is also a function of the working electrode; MacFarlane et al.[9,10] and Gonçalves and coworkers[11] observed that the reductive and oxidative decomposition of RTILs is dependent on the electrode material but did not consider mercury electrodes. Zhang and Bond[12] studied the electrochemical window of numerous ionic liquids and more conventional solvents on gold, glassy carbon, and platinum working electrodes, and it was noted (for $[C_4mim][BF_4]$) that the magnitude of the electrochemical reductive window adheres to the electrode material sequence of Au ≈ GC > Pt. The oxidation window magnitude follows the order Au > GC ≈ Pt.

This present article is a study seeking to develop the work by MacFarlane et al. and follows on from recent work by O'Mahony et al.,[5] which is a comprehensive examination of potential windows at platinum electrodes. Herein we report the fabrication of mercury hemispheres on platinum planar microdisc electrodes and assess the accessible electrochemical potential windows of various RTILs at the mercury droplet.

2. Experimental Section

2.1. Chemical Reagents. Mercury(I) nitrate dihydrate ($Hg_2(NO_3)_2$, Aldrich, 0.01 M), potassium nitrate (KNO_3, Aldrich, 99+ % ACS reagent, 0.10 M), nitric acid (HNO_3, Fisher Scientific, 70 %, 0.15 M), and ferrocene ($Fe(C_5H_5)_2$, Fc, Aldrich, 98 %) were all used as received. *n*-Hexyltriethylammonium bis(trifluoromethanesulfonyl)imide, $[N_{6,2,2,2}][NTf_2]$, and tri(*n*-hexyl)tetradecylphosphonium bis(trifluoromethanesulfonyl)imide, $[P_{14,6,6,6}][NTf_2]$, were prepared following standard literature procedures[8] using *n*-hexyltriethylammonium bromide ($[N_{6,2,2,2}]$-Br, Aldrich, 99 %) and tri(*n*-hexyl)tetradecylphosphonium chloride ($[P_{14,6,6,6}]Cl$, Cytec), respectively, for metathesis with lithium bis(trifluoromethanesulfonyl)imide, $Li[NTf_2]$.[8,13] 1-Ethyl-3-methylimidazolium bis(trifluoromethanesulfonyl)imide, $[C_2mim][NTf_2]$, 1-butyl-3-methylimidazolium bis(trifluoromethanesulfonyl)imide, $[C_4mim][NTf_2]$, *N*-butyl-*N*-methylpyrrolidinium bis(trifluoromethanesulfonyl)imide, $[C_4mpyrr][NTf_2]$, and their bromide salt precursors were prepared according to standard literature procedures.[8,14] Tri(*n*-hexyl)tetradecylphosphonium trifluorotris(pentafluoroethyl)phosphate, $[P_{14,6,6,6}][FAP]$, 1-butyl-3-methylimidazolium bis(trifluoromethanesulfonyl)imide tetrafluoroborate, $[C_4mim][BF_4]$, and 1-butyl-3-methylimidazolium bis(trifluoromethanesulfonyl)imide hexafluorophosphate, $[C_4mim][PF_6]$, were kindly donated by Merck KGaA and used as received. 1-Butyl-3-methylimidazolium trifluoromethane-

* Corresponding author. E-mail: richard.compton@chem.ox.ac.uk. Tel: +44(0) 1865 275 413. Fax: +44(0) 1865 275 410.
[†] Oxford University.
[‡] University of Belgrade.
[§] Queen's University Belfast.

10.1021/je800898z CCC: $40.75 © 2009 American Chemical Society
Published on Web 04/23/2009

Table 1. Illustrative Water Contents for Vacuum-Dried RTILs Used in This Study at 298 K[a]

ionic liquid	water content (ppm)
$[N_{6,2,2,2}][NTf_2]$	167
$[C_2mim][NTf_2]$	105
$[C_4mpyrr][NTf_2]$	133
$[C_4mim][NTf_2]$	144
$[C_4mim][BF_4]$	119
$[C_4mim][PF_6]$	268
$[C_4mim][OTf]$	250

[a] Data taken from work published previously,[5] obtained from Karl Fisher titrations.

sulfonate, $[C_4mim][OTf]$, was also kindly donated by Merck KGaA but was first diluted with CH_2Cl_2 before being passed through a column consisting of alternating layers of neutral aluminum oxide and silica gel to remove residual acidic impurities. 1-Butyl-3-methylimidazolium nitrate, $[C_4mim][NO_3]$, was synthesized using a method adapted from a previously published procedure.[15] Silver nitrate ($AgNO_3$, 5.36 g, 0.032 M) and 1-butyl-3-methylimidazolium chloride ($[C_4mim]Cl$, 5.00 g, 0.029 M) were dissolved separately in minimum amounts of ultrapure water, and $[C_4mim]Cl$ was slowly added to the stirred $AgNO_3$ solution. The resulting solution was stirred overnight and filtered to remove AgCl precipitate before the residual water was removed and the RTIL was dried at 70 °C under vacuum overnight. IL was then dissolved in 400 mL of dry methanol, and small amounts of activated charcoal and acidic alumina were added as seeds for remaining AgCl, and the solution was left overnight in the freezer. The solution was filtered, and the process was repeated. Methanol was removed, and IL was dried under high vacuum conditions. 1-Butyl-3-methylimidazolium methylsulfate, $[C_4mim][MeSO_4]$, was prepared according to a previously published procedure.[16] The water contents of the vacuum-dried RTILs are given in Table 1.

We made a mercury ion solution, from which the mercury droplet was deposited, by dissolving 0.1403 g mercury(I) nitrate dihydrate, $Hg_2(NO_3)_2$, 0.2527 g potassium nitrate, KNO_3 and 0.17 mL of nitric acid, HNO_3, in 25 mL of pure water, which was sonicated until all solid had dissolved.

We made the ferrocene solution used as an internal standard by dissolving 0.0186 g in 25 mL of acetonitrile.

2.2. Instrumental. A computer-controlled μ-Autolab potentiostat (Eco-Chemie, Netherlands) was used to undertake all electrochemical experiments. A mercury hemisphere was deposited from a mercury ion solution onto a planar platinum microelectrode using chronoamperometric methods. A 15 mL vial was used as the cell with a 15 mm thick PTFE lid containing four holes, one for each of the three electrodes (working, reference, and counter) and one for a nitrogen line. A 10 μm diameter platinum microelectrode was used as the working electrode with a 0.5 mm diameter silver wire reference electrode and a coiled platinum counter electrode. Before the mercury deposition procedure was undertaken, the platinum electrode was polished using (3.0, 1.0, and 0.1) μm diamond spray on soft lapping pads (Kemet, U.K.), and the mercury solution was bubbled with nitrogen gas (BOC, Guildford, Surrey, U.K.) for 30 min to remove atmospheric oxygen. We deposited mercury chronoamperometrically by holding the potential at −0.245 V for ca. 35 s.

To measure the potential windows of each ionic liquid, a two-elecrode arrangement was used with a mercury hemisphere on platinum working electrode and a silver wire (0.5 mm diameter) quasi-reference electrode. Because of an observed potential shift as a result of using a quasi-reference, a ferrocene internal reference was used.[10,12,17] The working electrode was modified with a plastic collar (section of disposable pipet tip) to form a cavity, into which 20 μL of RTIL was added with 20 μL of (i.e., 10 mM) ferrocene solution. The electrodes were housed in a T-cell (previously reported),[18] which allowed the liquid to be purged under vacuum prior to and during cyclic voltammetric measurements because oxygen is electroactive in these media.[19] Experiments were completed at 298 K in a heated Faraday cage.

3. Results and Discussion

Figure 1 shows the structures of the cations and anions that make up the RTILs chosen for this study. Many of the liquids have common cations or anions, which allowed us to determine the effect of varying certain cations/anions and to see if the potential window reflects simply the oxidation of the anions or the reduction of the constituent cations of the RTIL. As will become apparent below, this is not the case; rather, both the cation and anion identity influence each potential window.

Prior to investigation of the potential window of each liquid, the surface of the platinum electrode was renewed by polishing, and a new mercury droplet was deposited using the method described in Section 2.2.

Initially, we tested the deposition process by examining the redox behavior of the blank RTIL $[N_{6,2,2,2}][NTf_2]$. The resulting

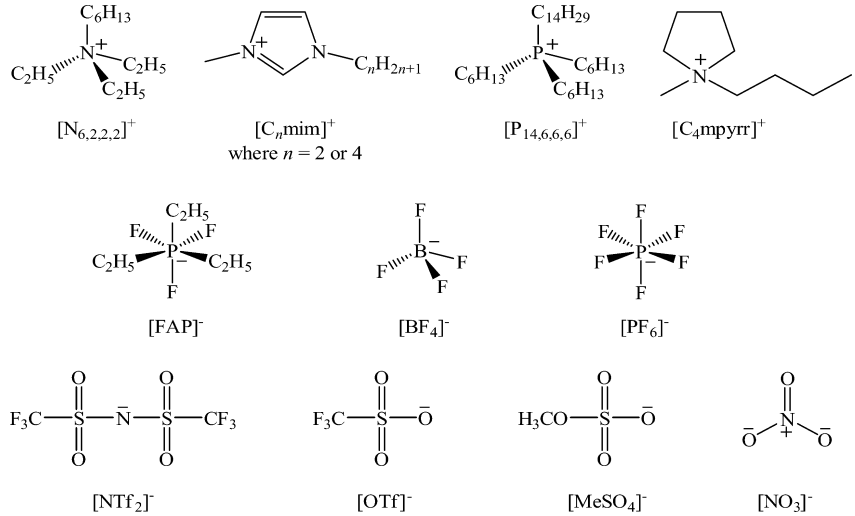

Figure 1. Structure of the cations and anions used in this study.

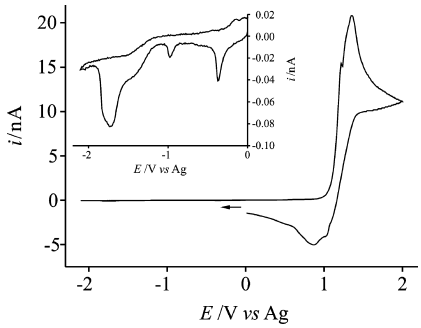

Figure 2. Cyclic voltammogram to show the stripping of the Hg droplet from the Pt microdisk at 100 mV·s^{-1} in [$N_{6,2,2,2}$][NTf_2]. The charge under the stripping peak was determined to be 1.24·10^{-7} C. Shown as an inset is the reductive window of [$N_{6,2,2,2}$][NTf_2] (not to breakdown potential).

Table 2. Cathodic Potential Limits versus Fc|Fc$^+$ for Various RTILs on a Mercury Electrode at Defined Current Densities

	RTIL 'breakdown' potentials (V) at defined current densities		
ionic liquid	250 μA·cm^{-2}	275 μA·cm^{-2}	320 μA·cm^{-2}
[$N_{6,2,2,2}$][NTf_2]	−3.508	−3.507	
[C_2mim][NTf_2]	−2.052	−2.079	−2.124
[$P_{14,6,6,6}$][NTf_2]	−3.117	−3.140	−3.160
[$P_{14,6,6,6}$][FAP]	−3.529	−3.538	−3.552
[C_4mpyrr][NTf_2]	−3.191	−3.198	−3.199
[C_4mim][NTf_2]	−2.455	−2.482	−0.493
[C_4mim][BF_4]	−2.472	−2.494	−2.515
[C_4mim][PF_6]	−2.379	−2.423	−2.454
[C_4mim][NO_3]	−1.654	−1.735	−1.886
[C_4mim][OTf]	−1.475	−1.496	−1.537
[C_4mim][$MeSO_4$]	−2.076	−2.084	

cyclic voltammogram in the absence of an internal reference is shown in Figure 2. The potential was scanned from (0.00 to −2.10) V and then back to + 2.00 V at 100 mV·s^{-1}. The inset

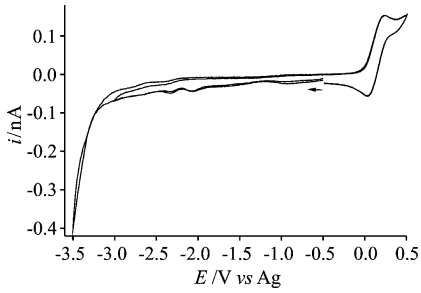

Figure 3. Cyclic voltammogram for the reductive window of [$N_{6,2,2,2}$][NTf_2] on a Hg electrode versus a Fc|Fc$^+$ internal reference, scanned from (−0.50 → −3.50 → + 0.50) V, at 100 mV·s^{-1}.

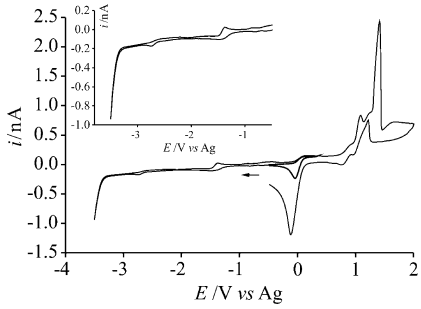

Figure 4. CV for the redox behavior of [$P_{14,6,6,6}$][FAP] scanned from (−0.50 → −3.5 → + 2.00) V at 100 mV·s^{-1} showing the reductive window (also shown as an inset) and the stripping peak of the Hg droplet from Pt microdisk. The oxidation of Fc is shown by the thick line ((−0.50 → + 0.50) V).

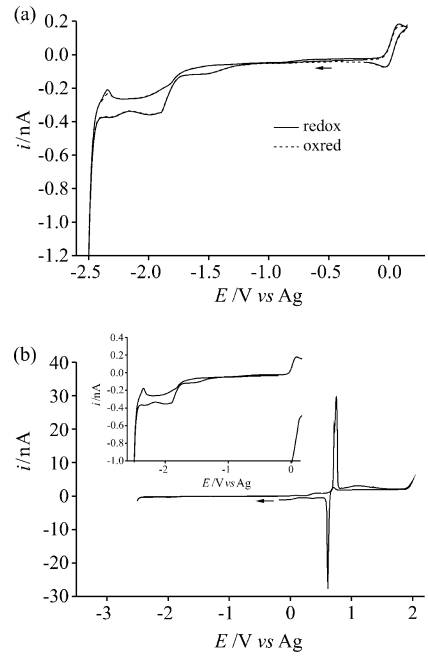

Figure 5. Cyclic voltammetry for (a) the reductive window and (b) the redox window of [C_4mim][BF_4] at a mercury electrode versus Fc|Fc$^+$. The potential was scanned from (−0.50 to −2.50) V and back to (a) + 0.15 V and (b) + 2.00 V. The scan rate used was 100 mV·s^{-1}.

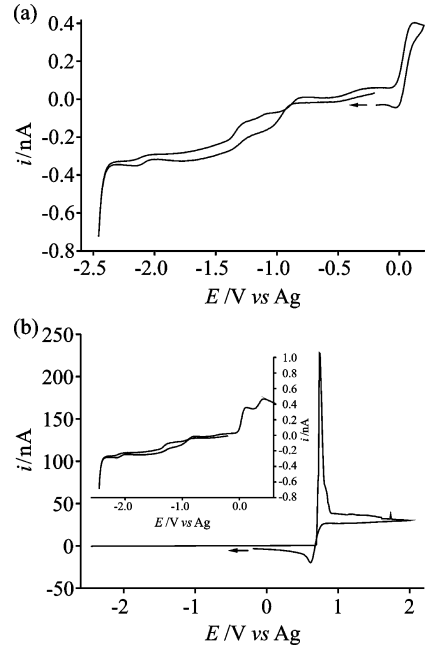

Figure 6. (a) Cyclic voltammogram for the reductive window of [C_4mim][NTf_2] versus Fc|Fc$^+$ at 100 mV·s^{-1} on a mercury hemisphere. (b) Cyclic voltammogram showing the cathodic and anodic window of [C_4mim][NTf_2] at 100 mV·s^{-1}.

to the Figure shows the reductive window ((0.00 to −2.10) V), which is essentially the background current related to this particular ionic liquid, although in this case, the potential is not at the cathodic limit of the liquid. In the oxidative region, a sharp peak is observed at ca. + 1.15 V versus Ag, which corresponds to the "stripping" of the mercury hemisphere from the planar Pt electrode, (Hg − e$^-$ → $^1/_2$ Hg_2^{2+}).

The next step in the investigation was to determine the reductive and oxidative windows of the various ionic liquids. To allow comparison of the potential limits, we added a ferrocene|ferrocenium (Fc|Fc$^+$) internal standard to the ionic

Table 3. Anodic Potential Limits versus Fc|Fc$^+$ for Various RTILs on a Mercury Electrode at Defined Current Densities

	Hg stripping potentials (V) at defined current densities (μA·cm^{-2}) in various RTILs													
ionic liquid	300	500	750	1000	1500	2000	3000	4000	5000	6000	7000	8000	9000	10 000
[$N_{6,2,2,2}$][NTf_2]	+ 0.996	+ 1.028	+ 1.048	+ 1.067	+ 1.088	+ 1.105	+ 1.128	+ 1.141	+ 1.153	+ 1.163	+ 1.171	+ 1.179	+ 1.193	+ 1.236
[C_2mim][NTf_2]	+ 0.776	+ 0.825	+ 0.834	+ 0.843	+ 0.846	+ 0.848	+ 0.852	+ 0.855	+ 0.857	+ 0.857	+ 0.859	+ 0.860	+ 0.862	+ 0.864
[$P_{14,6,6,6}$][NTf_2]	+ 1.471	+ 1.579	+ 1.721	+ 1.881	+ 2.478									
[$P_{14,6,6,6}$][FAP]	+ 0.750	+ 0.934	− 1.109	+ 1.161	+ 1.231	+ 1.293	+ 1.330							
[C_4mpyrr][NTf_2]	+ 0.168	+ 0.297	+ 0.313	+ 0.317	+ 0.322	+ 0.324	+ 0.329	+ 0.335	+ 0.344	+ 0.347	+ 0.353	+ 0.359	+ 0.378	+ 0.406
[C_4mim][NTf_2]	+ 0.633	+ 0.638	+ 0.645	+ 0.647	+ 0.647	+ 0.649	+ 0.649	+ 0.651	+ 0.651	+ 0.651	+ 0.651	+ 0.652	+ 0.653	+ 0.654
[C_4mim][BF_4]		+ 0.455	+ 0.584	+ 0.621	+ 0.636	+ 0.640	+ 0.645	+ 0.648	+ 0.651	+ 0.653	+ 0.654	+ 0.654	+ 0.658	+ 0.658
[C_4mim][PF_6]			+ 0.523	+ 0.535	+ 0.546	+ 0.551	+ 0.559	+ 0.567	+ 0.580	+ 0.627	+ 0.657	0.709		
[C_4mim][NO_3]	+ 0.150	+ 0.156	+ 0.162	+ 0.168	+ 0.168	+ 0.182	+ 0.190	+ 0.190	+ 0.190	+ 0.197	+ 0.203	+ 0.203	+ 0.203	+ 0.214
[C_4mim][OTf]		+ 0.291	+ 0.322	+ 0.333	+ 0.346	+ 0.355	+ 0.367	+ 0.375	+ 0.381	+ 0.385	+ 0.388	+ 0.388	+ 0.392	+ 0.394
[C_4mim][$MeSO_4$]			+ 0.213	+ 0.277	+ 0.302	+ 0.310	+ 0.316	+ 0.319	+ 0.321	+ 0.323	+ 0.324	+ 0.324	+ 0.325	+ 0.329

liquid.[10,12] First, we investigated the redox behavior of each liquid on the mercury electrode by scanning from either (0.00 or −0.50) V (depending on the potential of the ferrocene couple) to a potential where the reduction current, assumed to be due to the reduction of the cation, begins to increase above the baseline current. The potential was then scanned back to a point after the oxidation peak of ferrocene. The cathodic potential limit was determined at defined current density values, and Table 2 summarizes the results. The potentials quoted are related to Fc|Fc$^+$ and therefore correspond to the 'breakdown' potential of the RTIL versus Fc|Fc$^+$. Voltammetry was also undertaken in the absence of a ferrocene internal standard (not shown), and it was observed that the relative potential limits recorded were essentially the same as those in the presence of ferrocene. This suggests that the presence of the peaks relating to the redox couple had no effect on the solvent breakdown potentials at the ferrocene concentrations used. An example of the voltammogram observed is shown in Figure 3 for [$N_{6,2,2,2}$][NTf_2] on a Hg electrode versus Fc|Fc$^+$ at 100 mV·s^{-1}. From Table 2, the ionic liquid that gives the largest reductive window is [$P_{14,6,6,6}$][FAP], which was also observed by O'Mahony et al.,[5] who determined that this RTIL has a redox window of (4.2 to 5.4) V (vs Fc|Fc$^+$) on a 10 μm diameter platinum electrode. The reductive limit of [$P_{14,6,6,6}$][FAP] on mercury is comparable in magnitude to that of [$N_{6,2,2,2}$][NTf_2], both with a reductive limit larger than 3.50 V versus Fc|Fc$^+$. [C_4mpyrr][NTf_2] and [$P_{14,6,6,6}$][NTf_2] have reductive windows of greater than 3.00 V versus Fc|Fc$^+$, followed by the [$C_n$mim]$^+$ RTILs with potential windows between (2.48 and 1.48) V versus Fc|Fc$^+$, with [C_4mim][OTf] giving the smallest cathodic limit. A general trend can be determined: electrochemical reductive limit magnitude follows the cation sequence [$P_{14,6,6,6}$]$^+$ > [$N_{6,2,2,2}$]$^+$ > [C_4mpyrr]$^+$ > [$C_n$mim]$^+$. The [FAP]$^-$ and [NTf_2]$^-$ anions give larger windows than other anions (also observed by Ignat'ev et al.[20]) following the sequence [FAP]$^-$ ≈ [NTf_2]$^-$ > [BF_4]$^-$ > [PF_6]$^-$ > [OTf]$^-$ > [$MeSO_4$]$^-$ > [NO_3]$^-$. As previously mentioned, the reductive limit is presumed to be determined by the reduction of the cation, so it would be expected that varying the cation of an ionic liquid with a common anion would provoke a variation in the reductive potential window depending on the stability of the cation to reduction. Looking at the cathodic limits of the liquids studied (Table 2) with the [NTf_2]$^-$ anion (at a current density of 250 μA·cm^{-2}) and various cations, we observe a 1.50 V difference in the reductive potential limit, ranging from 3.51 V versus Fc|Fc$^+$ for [$N_{6,2,2,2}$]$^+$ to 2.05 V versus Fc|Fc$^+$ for [C_2mim]$^+$. It should be noted that when looking at the cathodic limits for ILs with a common cation ([C_4mim]$^+$) and varying the anion, a difference of 1.00 V in the potential window limit is observed, from 2.47 V versus Fc|Fc$^+$ for [BF_4]$^-$ to 1.48 V versus Fc|Fc$^+$ for [OTf]$^-$. This suggests that although the cation affects the accessible reductive limit, the identity of the anion also plays a role in the 'breakdown' potential of the ionic liquid.

Following this, the oxidative limit was determined for the same ionic liquids. The potential was cycled from either (0.00 or −0.50) V to a point after the cathodic limit and then cycled oxidatively to + 2.00 V to show the ferrocene couple and the stripping of the Hg droplet from the Pt surface. Figure 4 shows the voltammetry observed for [$P_{14,6,6,6}$][FAP] and 10 mM Fc at the Hg electrode at 100 mV·s^{-1}. The oxidative window shows the oxidation of ferrocene, followed by the stripping of Hg from a potential of ca. + 0.75 V. This method allows determination of the anodic limit, normally attributed to the oxidation of the anion, but in this case, the anodic limit of the window is due to the stripping of Hg from Pt. The stripping peak shown in Figure 4 differs from that observed in Figure 2, as it does for many of the RTILs in this study, and this is most likely due to an overlap with the anodic breakdown of the ionic liquid. Figures 5 and 6 show voltammetry for (a) the reductive window versus Fc|Fc$^+$ and (b) the reductive and oxidative window versus Fc|Fc$^+$ for [C_4mim][BF_4] and [C_4mim][NTf_2], respectively. Again, differences in the stripping peak are observed with variation in the RTIL. The stripping potential/anodic limit of the window was determined at defined current densities, and Table 3 summarizes the results obtained when corrected for ferrocene, that is, stripping potential versus Fc|Fc$^+$. In this case, the widest oxidative limit is achieved by [$P_{14,6,6,6}$][NTf_2] (> 2.40 V vs Fc|Fc$^+$ at a current density of 1500 μA·cm^{-2}), with [C_4mim][NO_3] giving the smallest oxidative window (ca. 0.17 V vs Fc|Fc$^+$ at 1500 μA·cm^{-2}). Again, a general trend for the magnitude of the electrochemical oxidative limit is observed as follows: [$P_{14,6,6,6}$]$^+$ > [$N_{6,2,2,2}$]$^+$ > [$C_n$mim]$^+$ ≈ [C_4mpyrr]$^+$ and [FAP]$^-$ ≈ [NTf_2]$^-$ > [BF_4]$^-$ > [PF_6]$^-$ > [$MeSO_4$]$^-$ > [NO_3]$^-$ > [OTf]$^-$. The anodic "breakdown" is presumed to be due to the oxidation of the anionic component of the RTIL. Looking at the anodic potential limits (at a current density of 1500 μA·cm^{-2}) for liquids with the common [NTf_2]$^-$ anion, a potential difference of ca. 2.20 V was observed when the cation was varied between [$P_{14,6,6,6}$]$^+$ (2.48 V vs Fc|Fc$^+$) and [C_4mpyrr]$^+$ (0.32 V vs Fc|Fc$^+$). The variation in the anion is expected to provoke more of a deviation in the accessible potential window. From Table 3, it is observed that the largest oxidative window was 0.65 V versus Fc|Fc$^+$ for [C_4mim][NTf_2], and the smallest window was 0.17 V versus Fc|Fc$^+$ for [C_4mim][NO_3], that is, a 500 mV difference in the anodic potential limit for a common cation and various anions. The results confirm that it is not simply a case of the reduction of the cation and the oxidation of the anion that determines the cathodic and anodic potential windows. In this system, it is more likely that the anodic window is determined by the stripping of Hg from Pt, the potential of which also varies between ionic liquids.

4. Conclusions

The potential windows of eleven different ionic liquids have been determined electrochemically at a mercury hemisphere electrode. The reductive and oxidative potential limits have been reported versus the ferrocene|ferrocenium ($Fc|Fc^+$) couple, and it was observed that the phosphonium cation (tri(*n*-hexyl)tetradecylphosphonium, $[P_{14,6,6,6}]^+$), combined with trifluorotris(pentafluoroethyl)phosphate, $[FAP]^-$, or bis(trifluoromethanesulfonyl)imide, $[NTf_2]^-$, gives the largest potential windows.

Acknowledgment

E.I.R. thanks Dr. Neil Rees and Mr. Juan Gualberto Limon Petersen for help with the mercury deposition procedure. B.S. thanks St. John's College, Oxford for hospitality over the summer of 2008.

Literature Cited

(1) Silvester, D. S.; Compton, R. G. Electrochemistry in Room Temperature Ionic Liquids: A Review and Some Possible Applications. *Z. Phys. Chem.* **2006**, *220*, 1247–1274.
(2) Buzzeo, M. C.; Evans, R. G.; Compton, R. G. Non-Haloaluminate Room Temperature Ionic Liquids in Electrochemistry: A Review. *ChemPhysChem* **2004**, *5*, 1106–1120.
(3) Earle, M. J.; Seddon, K. R. Ionic Liquids. Green Solvents for the Future. *Pure Appl. Chem.* **2000**, *72*, 1391–1398.
(4) Endres, F.; Zein El Abedin, S. Air and Water Stable Ionic Liquids in Physical Chemistry. *Phys. Chem. Chem. Phys.* **2006**, *8*, 2101–2116.
(5) O'Mahony, A.; Silvester, D. S.; Aldous, L.; Hardacre, C.; Compton, R. G. Effect of Water on the Electrochemical Window and Potential Limits of Room-Temperature Ionic Liquids. *J. Chem. Eng. Data* **2008**, *53*, 2884–2891.
(6) Buzzeo, M. C.; Hardacre, C.; Compton, R. G. Extended Electrochemical Windows Made Accessible by Room Temperature Ionic Liquid/Organic Solvent Electrolyte Systems. *ChemPhysChem* **2006**, *7*, 176–180.
(7) Fitchett, B. D.; Knepp, T. N.; Conboy, J. C. 1-Alkyl-3-methylimidazolium Bis(perfluoroalkylsulfonyl)imide Water-Immiscible Ionic Liquids. *J. Electrochem. Soc.* **2004**, *151*, E219–E224.
(8) Bonhôte, P.; Dias, A.-P.; Papageorgiou, N.; Kalyanasundaram, K.; Grätzel, M. Hydrophobic, Highly Conductive Ambient-Temperature Molten Salts. *Inorg. Chem.* **1996**, *35*, 1168–1178.
(9) Howlett, P. C.; Izgorodina, E. I.; Forsyth, M.; MacFarlane, D. R. Electrochemistry at Negative Potentials in Bis(trifluormethanesulfonyl)amide Ionic Liquids. *Z. Phys. Chem.* **2006**, *220*, 1483–1498.
(10) Zhao, C.; Burrell, G.; Torriero, A. A. J.; Separovic, F.; Dunlop, N. F.; MacFarlane, D. R.; Bond, A. M. Electrochemistry of Room Temperature Protic Ionic Liquids. *J. Phys. Chem. B* **2008**, *112*, 6923–6936.
(11) Suarez, P. A. Z.; Consorti, C. S.; de Souza, R. F.; Dupont, J.; Gonçalves, R. S. Electrochemical Behaviour of Vitreous Glass Carbon and Platinum Electrodes in the Ionic Liquid 1-*n*-Butyl-3-methylimidazolium Trifluoroacetate. *J. Braz. Chem. Soc.* **2002**, *13*, 106–109.
(12) Zhang, J.; Bond, A. M. Practical Considerations Associated with Voltammetric Studies in Room Temperature Ionic Liquids. *Analyst* **2005**, *130*, 1132–1147.
(13) Ge, R.; Hardacre, C.; Nancarrow, P.; Rooney, D. W. Thermal Conductivities of Ionic Liquids over the Temperature Range from 293 K to 353 K. *J. Chem. Eng. Data* **2007**, *52*, 1819–1823.
(14) MacFarlane, D. R.; Meakin, P.; Sun, J.; Amini, N.; Forsyth, M. Pyrrolidinium Imides: A New Family of Molten Salts and Conductive Plastic Crystal Phases. *J. Phys. Chem. B* **1999**, *103*, 4164–4170.
(15) Cammarata, L.; Kazarian, S. G.; Salter, P. A.; Welton, T. Molecular States of Water in Room Temperature Ionic Liquids. *Phys. Chem. Chem. Phys.* **2001**, *3*, 5192–5200.
(16) Pereiro, A. B.; Santamarta, F.; Tojo, E.; Rodriguez, A.; J. Tojo, J. Temperature Dependence of Physical Properties of Ionic Liquid 1,3-Dimethylimidazolium Methyl Sulfate. *J. Chem. Eng. Data* **2006**, *51*, 952–954.
(17) Rogers, E. I.; Silvester, D. S.; Poole, D. L.; Aldous, L.; Hardacre, C.; Compton, R. G. Voltammetric Characterisation of the Ferrocene|Ferrocenium and Cobaltocenium|Cobaltocene Redox Couples in RTILs. *J. Phys. Chem. C* **2008**, *112*, 2729–2735.
(18) Schröder, U.; Wadhawan, J. D.; Compton, R. G.; Marken, F.; Suarez, P. A. Z.; Consorti, C. S.; de Souza, R. F.; Dupont, J. Water-Induced Accelerated Ion Diffusion: Voltammetric Studies in 1-Methyl-3-[2,6-(*S*)-dimethylocten-2-yl]imidazolium Tetrafluoroborate, 1-Butyl-3-methylimidazolium Tetrafluoroborate and Hexafluorophosphate Ionic Liquids. *New J. Chem.* **2000**, *24*, 1009–1015.
(19) Buzzeo, M. C.; Klymenko, O. V.; Wadhawan, J. D.; Hardacre, C.; Seddon, K. R.; Compton, R. G. Voltammetry of Oxygen in the Room-Temperature Ionic Liquids 1-Ethyl-3-methylimidazolium Bis((trifluoromethyl)sulfonyl)imide and Hexyltriethylammonium Bis((trifluoromethyl)sulfonyl)imide: One-Electron Reduction To Form Superoxide. Steady-State and Transient Behavior in the Same Cyclic Voltammogram Resulting from Widely Different Diffusion Coefficients of Oxygen and Superoxide. *J. Phys. Chem. A* **2003**, *107*, 8872–8878.
(20) Ignat'ev, N. V.; Welz-Biermann, U.; Kucheryna, A.; Bissky, G.; Willner, H. New Ionic Liquids with Tris(perfluoroalkyl)trifluorophosphate (FAP) Anions. *J. Fluorine Chem.* **2005**, *126*, 1150–1159.

Received for review November 24, 2008. Accepted March 22, 2009. E.I.R thanks EPSRC for financial support.

JE800898Z